Characterization of the mitochondrial genome of *Tetrameres grusi* and insights into the phylogeny of Spirurina

Jun-Feng Gao [a], Rui-Feng Mao [a], Ye Li [b], Yun-Yi Sun [a], Zhong-Yan Gao [c], Xian-Guang Zhang [c], Zhen-Hua Jin [b], Qi An [a], Zhong-Huai Zhang [a], Ai-Hui Zhang [a], Wei Wei [a], Zhuo Lan [a], Chun-Ren Wang [a,*]

[a] *College of Animal Science and Veterinary Medicine, Heilongjiang Bayi Agricultural University, Daqing, 163319, Heilongjiang Province, China*
[b] *Branch of Animal Husbandry and Veterinary of Heilongjiang Academy of Agricultural Sciences, Qiqihar, Heilongjiang Province, 161005, China*
[c] *Heilongjiang Zhalong National Natural Reserve Administration, Qiqihar, 161000, Heilongjiang Province, China*

ABSTRACT

Tetrameres grusi is a significant parasitic nematode of cranes that is classified into suborder Spirurina. However, for more than a century, this classification has been controversial. Mitochondrial genomes are valuable resources for parasite taxonomy, population genetics and systematics studies. Here, the mitochondrial genome of *T. grusi* was determined and subsequently compared with those from Spirurina species using concatenated datasets of amino acid sequences predicted from mitochondrial protein-coding genes. The complete mitochondrial genome of *T. grusi* is circular with 13,709 bp, and it contains 12 protein-coding genes, 22 transfer RNA genes, two ribosomal RNA genes and one non-coding region. All of the protein-coding genes are transcribed in the same direction. There were 18 intergenic spacers of 1–44 bp, and six locations with gene overlaps, ranging from 1 bp to 28 bp, in the mitochondrial genome of *T. grusi*. The AT content of this mitochondrial genome was 71.56%. This was similar to mitochondrial genomes of other Spirurina species, which also exhibited strong AT content bias, not only in the nucleotide composition but also in codon usage. The sequenced mitogenomes of the 25 Spirurina nematodes showed three classes of gene arrangements based on the 12 protein-coding genes, and the gene arrangement of the *T. grusi* mitochondrial genome belonged to the Class I. Phylogenetic analyses using mitochondrial genomes of 25 Spirurina nematodes revealed that *T. grusi* (Habronematoidea) was closer to *Gongylonema pulchrum* (Spiruroidea) than *Spirocerca lupi* (Thelazioidea). The availability of the complete mitochondrial genome sequence of *T. grusi* provides new and useful genetic markers for further studies on Spirurina nematodes.

1. Introduction

Suborder Spirurina nematodes belong to order Spirurida, which is divided into 10 superfamilies, including Acuarioidea, Aproctoidea, Camallanoidea, Diplotriaenoidea, Filarioidea, Habronematoidea, Lucionematoidea, Rictularioidea, Spiruroidea, and Thelazioidea (de Ley and Blaxter, 2004; Hodda, 2011). Due to the species-rich in suborder Spirurina, including a heterogeneous group of nematodes. The phylogeny of suborder Spirurina nematodes are controversial and have been revised several times in recent years, especially the application of rDNA in molecular classification (Honisch and Krone, 2008).

Tetrameres nematodes are the important members of suborder Spirurina nematodes, which known as the 'avian stomach nematodes'.

Tetrameres nematodes are the etiological agents of tetrameriosis in poultry, and they may also infest wild birds, including penguin (Fink et al., 2004; González-Acuña et al., 2020; Werneck et al., 2020). Mature female worms are blood-red colored with a special subspherical morphology, as they lie embedded in the crypts of Lieberkühn while feeding on blood. In contrast, the male worms are white and live freely in the lumen of the proventriculus (Soulsby, 1982). Tetrameriosis can cause severe proventriculitis and reduces the secretion of digestive juices. It manifests into a debilitating state that is characterized by emaciation and anemic conditions. In heavily infected poultry the condition may lead to debilitation and wasting, and it may be fatal in migratory wild birds (Soulsby, 1982). The *Tetrameres* spp. have been frequently reported as being distributed worldwide (Agüero et al., 2016).

Although there are many reported *Tetrameres* spp., such as *T. grusi* (Mowlavi et al., 2006), *T. mothedai* (Schou et al., 2007), *T. wetzeli* (Diaz et al., 2013), *T. pattersoni* (Olsen et al., 2016), *T. striata* (Amundson et al., 2016), *T. globosa* (Królaczyk et al., 2018), *T. americana* (Mukaratirwa and Khumalo, 2010), and *T. fissipina* (Padilla-Aguilar et al., 2020), only the partial nuclear small subunit (SSU) rRNA gene sequences of *T. grusi* and *T. fissipina* have been deposited in the NCBI GenBank nucleic acid sequence database. Moreover, the classification of *Tetrameres* spp. nematodes has been controversial, primarily at the genus level. Nadler et al. (2007) first reported the SSU rRNA sequences of *T. fissipina* and discussed the taxonomy and phylogenies of Clade III nematodes on the basis of the SSU rRNA sequences (Nadler et al., 2007). In phylogenetic trees, *T. fissipina* is closer to the Filariata than Spirurina nematodes, which result is inconsistent with morphological taxonomy. Thus, the phylogenetic relationships among genus *Tetrameres* nematodes remains unclear, and phylogenetic analyses are needed to reconstruct its evolutionary history.

Mitochondrial genomes (mitogenomes) have maternal inheritance, an apparent lack of recombination, rapid evolutionary rates and comparatively conserved genomic structures (Pyziel et al., 2020). Recently, sequences of whole mitogenomes have been used to infer phylogenetic relationships among parasites at different taxonomic levels (Gao et al., 2021). For example, mitogenome dataset-based phylogenetic analyses showed that *Parascaris equorum* and *Parascaris univalens* are very closely related compared with other ascarids, and these mitogenome datasets provide genetic evidence that *P. equorum* and *P. univalens* represent the same species (Gao et al., 2019). In addition, *Bunostomum trigonocephalum* and *Bunostomum phlebotomum* are significantly similar in morphology and biological characteristics, but whether they represent different species or strains has been controversial. Gao et al. (2014) used mitogenome datasets to show that *B. trigonocephalum* and *B. phlebotomum* represent distinct but closely-related species (Gao et al., 2014). However, the mitogenome-based phylogenetic position of *Tetrameres* nematodes was unknown until now.

Therefore, the objectives of the present study were to determine the complete mitogenome of *T. grusi*, the first representative species of the Habronematoidea, and to compare this mitogenome with those of other nematodes in suborder Spirurina. Finally, its phylogenetic relationships were determined on the basis of the mitogenome amino acid sequence data to assess the systematics of *T. grusi* and its phylogenetic position within the Spirurina.

2. Materials and methods

2.1. Parasites and total genomic DNA isolation

A one-year-old female red-crowned crane died in September 2020 in Heilongjiang Zhalong National Natural Reserve, Qiqihar, China (47°13′42″N, 124°14′17″E), an autopsy was performed on the dead red-crowned crane to determine the causes of death. Adult female specimens of *T. grusi* were collected from the glandular stomach of red-crowned crane follow the wildlife protection law of the People's Republic of China (a draft of an animal protection law in China released on 2018). Specimens were washed in physiological saline and identified morphologically to the species level (Mowlavi et al., 2006). They were then fixed in 75% ethanol and stored at −20 °C until used. Total genomic DNA was isolated from individual specimen using a sodium dodecyl sulphate/-proteinase K treatment, followed by spin-column purification (Wizard® Genomic DNA Purification System, Promega, WI, USA). To independently verify the identity of the specimen, the partial region of the SSU rRNA sequence was amplified from the genomic DNA using PCR with previously reported primers (Nadler et al., 2007). The region had a 100% identity with previously published sequences of *T. grusi* from *Grus canadensis* isolated in the USA (GenBank accession number **KX172117**).

2.2. Sequencing and mitogenome assembly

Illumina paired-end shotgun libraries were prepared using the standard protocol of the Nextera™ DNA Sample Prep Kit (Epicentre®) and sequenced using an Illumina NovaSeq sequencing platform (Shanghai Personal Biotechnology Co. Ltd. China) using 2 × 100 cycles. Raw sequences data were deposited into the Short Read Archive database (https://www.ncbi.nlm.nih.gov/sra/) under the accession number **PRJNA718647**. Clean data without sequencing adapters were de novo assembled using NOVOPlasty software (Dierckxsens et al., 2017). The completeness of the mitogenome assembly was further verified by PCR and Sanger sequencing using four pairs of primers that were designed on the basis of conserved regions (Table S1; Fig. S1).

2.3. Sequence analysis and gene annotation

Mitogenome sequences served as query for BLAST search of the NCBI database (http://blast.ncbi.nlm.nih.gov/Blast) (Altschul et al., 1997). The protein-coding genes (PCGs) were initially identified using "ORF Finder" through NCBI and the MITOS Web Server (Rombel et al., 2002) to specify the mitochondrial genetic code of invertebrates. The MITOS Web Server was used to calculate the potential stem-loop secondary structures within these tRNA gene sequences (Bernt et al., 2013). The codon usage of the 12 PCGs was analyzed using the invertebrate genetic code and the Codon Usage web server (http://www.bioinformatics.org/sms2/codon_usage.html). An analysis of compositional skews was conducted using the formulae (Perna and Kocher, 1995): AT-skew = (A − T)/(A + T) and GC-skew = (G − C)/(G + C). A gene map of the mitogenome was constructed using the online mitochondrial visualization tool OrganellarGenomeDRAW (Lohse et al., 2013).

2.4. Phylogenetic analyses

Phylogenies were constructed using the data from the 12 PCGs of representative Spirurina nematodes available in GenBank. In addition to the newly sequenced mitogenome of *T. grusi*, it contained the mitogenomes of *Brugia malayi* (NC_004298), *Brugia timori* (AP017686), *Brugia pahangi* (AP017680), *Wuchereria bancrofti* (NC_016186), *Loa loa* (NC_016199), *Acanthocheilonema viteae* (NC_016197), *Chandlerella quiscali* (NC_014486), *Mansonella perstans* (MT361687), *Setaria digitata* (NC_014282), *Setaria labiatopapillosa* (NC_044071), *Thelazia callipaeda* (NC_018363), *Heliconema longissimum* (GQ332423), *Gongylonema pulchrum* (NC_026687), *Spirocerca lupi* (KC305876), *Dirofilaria immitis* (NC_005305), *Dirofilaria repens* (NC_029975), *Onchocerca ochengi* (NC_031891), *Onchocerca volvulus* (NC_001861), *Onchocerca lupi* (MW266120), *Onchocerca flexuosa* (NC_016172), *Physaloptera rara* (MH931178), *Philometroides sanguineus* (NC_024931), *Dracunculus medinensis* (NC_016019), and *Camallanus cotti* (NC_036308) with *Bunostomum phlebotomum* (NC_012308) as an outgroup. Nucleotide sequences of each gene and corresponding deduced amino acid sequences were aligned using MUSCLE 3.8 (Edgar, 2004) in MEGA 11.0 (Tamura et al., 2021). The amino acid sequences for each of the 12 PCGs from the mitogenomes were aligned using the default settings and then concatenated. On the basis of the constructed phylogenetic trees, the taxonomic status of *T. grusi* within Spirurina was estimated.

Phylogenetic analyses were performed using the concatenated set of amino acid sequences. Bayesian Inference (BI) and Maximum Likelihood (ML) phylogenetic trees were obtained by using MrBayes v3.2.6 (Huelsenbeck and Ronquist, 2001) and RaxML v8.2.11 (Stamatakis, 2014), respectively. The best-fit substitution model for phylogenetic analysis of the amino acid alignment was determined, using jModeltest under AIC was the SYM+I+G model. (Darriba et al., 2012). BI analysis was conducted for 10,000,000 generations, in two simultaneous runs, with four chains (three heated and one cold), to catalyze swapping among the Markov-chain Monte Carlo chains. Trees were sampled every 1,000 generations. We used the software Tracer v1.6 (http://tree.bio.ed.ac.
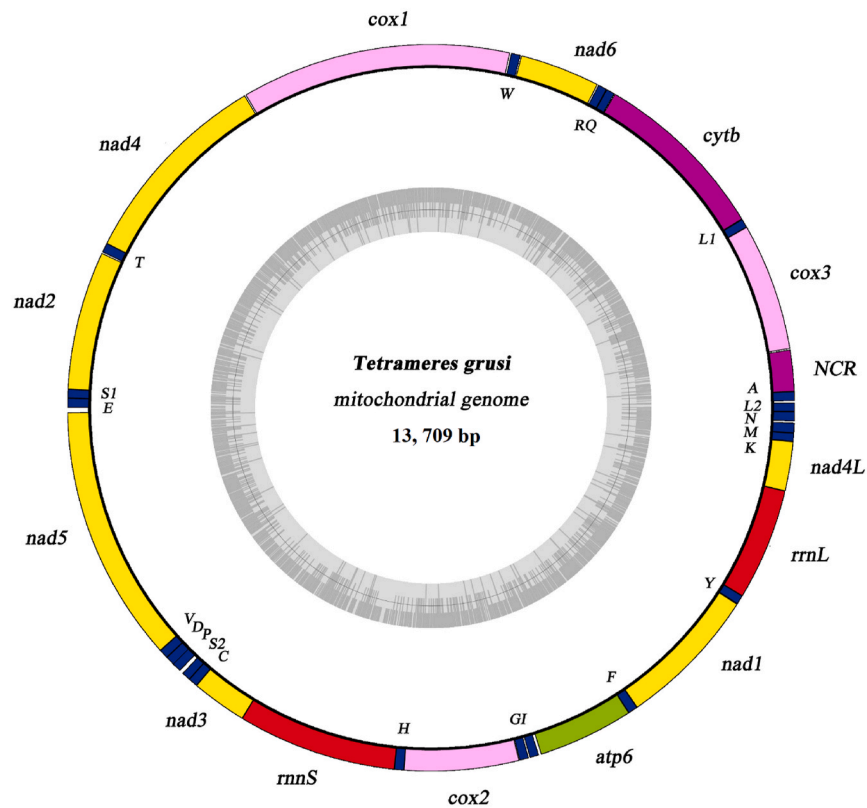
Fig. 1. Gene map of the mitogenome of *Tetrameres grusi*. PCGs are colour-coded (*cox*: lavender; *nad*: yellow; *atp*: green; *cyt*: purple); rRNAs are in red; tRNAs are in dark blue. Abbreviations of PCGs are: *atp*6 for ATP synthase subunits 6, *cox*1–3 for cytochrome oxidase subunits 1–3, *cyt*b for cytochrome b, *nad*1–6 and *nad*4L for NADH dehydrogenase subunits 1–6 and 4L, *rrn*L and *rrn*S for large and small rRNA subunits, 22 tRNAs are designated by the one-letter code for the corresponding amino acid, with numerals differentiating each of the two leucine and serine-specifying tRNAs (L1 and L2 for codon families CUN and UUR, respectively; S1 and S2 for codon families UCN and AGN, respectively), NCR refers to Non-coding region. All genes are transcribed in the clockwise direction.

uk/software/tracer/) to investigate the convergence of sampled parameters and potential autocorrelation (effective sample size (ESS) for all parameters >200). In addition, we checked the average standard deviations of the split frequencies between both runs (<0.01). Bayesian posterior probabilities were obtained from the 50% majority-rule consensus of the post-burn-in trees sampled at stationarity after removing the first 25% of trees as a "burn-in" stage. ML analysis was conducted for the GTRGAMMAI model and 1000 rapid bootstrapping replications were used to evaluate the bootstrap support values and search for the best ML tree. The final phylogenetic tree was graphically visualized and edited using FigTree v1.4.3 (http://tree.bio.ed.ac.uk/software/figtree/).

3. Results and discussion

3.1. General features of the mitogenome

The total *T. grusi* mitogenome (13,709 bp) is a closed circular molecule (GenBank accession number **MW648425**) that contains 12 PCGs (*cox*1–3, *nad*1–6, *nad*4L, *cyt*b, and *atp*6), 22 tRNA genes (one for each amino acid and two each for leucine and serine), two rRNA genes (*rrn*L and *rrn*S), and a major non-coding region (NCR), but lacks an *atp*8 gene (Fig. 1; Table 1). All the genes are transcribed in the same direction. There are 18 intergenic spacers, ranging from 1 to 44 bp, and six locations with gene overlaps, ranging from 1 to 28 bp, in the *T. grusi* mitogenome (Table 1). There is only one NCR, which is consistent with other related Spirurina species (Yatawara et al., 2010; Hu et al., 2003;

McNulty et al., 2012).

As observed in other Spirurina species, the nucleotide composition of the entire mitogenome of *T. grusi* is biased toward A and T, with an overall AT content of 71.56%. The low GC contents in these mitogenomes may be indicative of the high conservation of this genic structure. Genic structures with the fastest evolutionary rates have high GC contents, with the predominant replacements being G and C nucleotide insertions, resulting in divergence from the ancestral structure in metazoans (de Lima et al., 2017). The AT- and GC-skews of the selected complete mitogenome were calculated as −0.489 and 0.582, respectively. The negative AT-skew indicated a higher incidence of T than A nucleotides. The positive GC-skew indicated that G are more abundant than C. The AT-/GC-skews of the PCGs, rRNA and tRNAs were calculated for the entire *T. grusi* mitogenome (Table 2).

3.2. PCGs and codon usage

In the *T. grusi* mitogenome, the 12 PCGs accounted for 10,267 bp and encoded 3,413 amino acids, excluding the termination codons. The average AT content of the 12 PCGs was 69.8%. Moreover, the AT-skew of the PCGs was negative, whereas the GC-skew was positive (Table 2). A common feature of mitogenomes in most metazoans is a bias toward a higher representation of the A and T nucleotides, which leads to subsequent biases in the corresponding encoded amino acids (Hu et al., 2020).

The initiation and termination codons of the PCGs in the *T. grusi* mitogenome are listed in Table 1. The most common initiation codon for

Table 1
Features of the mitogenome of *Tetrameres grusi*.

Genes	Location	Length (bp)	Initiation codons	Termination codons	Anticodons	Intergenic spacers (bp)
*cox*1	1–1656	1656	ATG	TAG		5
*trn*W	1662–1717	56			TCA	44
*nad*6	1762–2206	445	ATT	T		0
*trn*R	2207–2260	54			ACG	1
*trn*Q	2262–2316	55			TTG	32
*cyt*b	2349–2404	1056	TTG	TAG		5
*trn*L1	3409–3465	57			TAG	2
*cox*3	3468–4244	777	ATT	TAG		0
NCR	4245–4611	367				0
*trn*A	4612–4672	61			TGC	2
*trn*L2	4675–4728	54			TAA	0
*trn*N	4729–4786	58			GTT	1
*trn*M	4788–4845	58			CAT	2
*trn*K	4848–4904	57			CTT	3
*nad*4l	4908–5138	231	TTG	TAA		0
*rrn*S	5139–5830	687				0
*trn*Y	5826–5880	55			GTA	0
*nad*1	5881–6753	873	ATA	TAG		1
*trn*F	6755–6814	60			GAA	3
*atp*6	6818–7393	576	TTG	TAG		5
*trn*I	7399–7451	53			GAT	2
*trn*G	7454–7512	59			TCC	0
*cox*2	7513–8205	693	TTG	TAA		0
*trn*H	8206–8262	57			GTG	0
*rrn*L	8262–9223	961				0
*nad*3	9224–9563	340	TTG	T		0
*trn*C	9564–9621	58			GCA	0
*trn*S2	9622–9678	57			TGA	0
*trn*P	9679–9739	61			AGG	19
*trn*D	9759–9814	56			GTC	8
*trn*V	9823–9878	56			TAC	9
*nad*5	9888-11,472	1585	TTG	T		0
*trn*E	11,473–11,529	57			TTC	0
*trn*S1	11,530–11,580	51			TCT	18
*nad*2	11,599–12,415	817	TTG	T		0
*trn*T	12,416–12,473	58			TGT	17
*nad*4	12,491–13,708	1218	TTG	TAA		1

Table 2
Nucleotide composition of 12 PCGs, rRNAs, and NCR of *Tetrameres grusi*. DNA base composition is shown as percentages.

	Size(bp)	A(%)	T(%)	G(%)	C(%)	A+T(%)	AT-skew	GC-skew
Mitogenome	13,709	18.29	53.26	21.73	6.71	71.56	−0.489	0.528
PCGs	10,267	15.56	54.23	23.02	7.19	69.8	−0.554	0.524
*atp*6	576	13.02	59.72	21.01	6.25	72.74	−0.642	0.541
*cox*1	1,656	18.54	46.07	24.46	10.93	64.61	−0.426	0.382
*cox*2	693	19.19	45.6	26.26	8.95	64.79	−0.408	0.492
*cox*3	777	17.76	49.03	25.48	7.72	66.8	−0.468	0.535
*nad*1	873	11.91	56.01	24.4	7.67	67.93	−0.649	0.522
*nad*2	817	14.44	57.41	22.77	5.39	71.85	−0.598	0.617
*nad*3	340	13.82	63.24	19.41	3.53	77.06	−0.641	0.692
*nad*4	1,218	14.70	55.67	23.07	6.57	70.36	−0.582	0.557
*nad*4L	231	13.42	61.9	21.21	3.46	75.32	−0.644	0.719
*nad*5	1,585	14.57	57.92	21.45	6.06	72.49	−0.598	0.559
*nad*6	445	13.03	62.25	22.92	1.8	75.28	−0.654	0.854
*cyt*b	1,056	16.76	54.45	20.83	7.95	71.21	−0.529	0.448
*rrn*S	687	27.07	48.18	17.9	6.84	75.25	−0.281	0.447
*rrn*L	961	23.83	52.86	17.59	5.72	76.69	−0.379	0.509
tRNA	1,248	29.01	47.76	18.11	5.13	76.76	−0.244	0.559
NCR	367	29.97	48.23	17.98	3.81	78.2	−0.234	0.650

T. grusi was TTG (8 of 12 PCGs), followed by ATT (2 of 12 PCGs), ATG (1 of 12 PCGs), and ATA (1 of 12 PCGs). Eight of 12 PCGs were predicted to have TAG (5) or TAA (3) as termination codons, and the incomplete termination codon T were present in 4 PCGs, which is consistent with sequences of other Spirurina, including *G. pulchru*m, *B. malayi*, *D. immitis*, *O. volvulus*, *W. bancrofti*, *L. loa*, *C. quiscali*, and *S. digitata*, although different from *S. lupi* (Liu et al., 2013).

The codon usage analyses of the 12 PCGs in the mitogenome is summarized in Table 3. The most frequently employed amino acid was Phe (TTT: 18.33%), followed by Leu (TTG; 9.27%), Val (GTT; 7.86%), and Tyr (TAT; 5.73%). The least frequently used codons were Leu (CTC, 0%) and Arg (CGA; 0%) (Table 3), which is consistent with previously published data (Deng et al., 2021a).

3.3. Transfer RNAs, ribosomal RNAs, and the NCR

The 22 tRNA genes identified in the *T. grusi* mitogenome ranged from 51 to 61 bp. The total length was 1,248 bp, and the AT content was

Table 3

Codon usage analysis of 12 PCGs in the mitochondrial genome of *Tetrameres grusis*.

| Codon	Number	/1000	Fraction	Codon	Number	/1000	Fraction
UUU(Phe)	627	183.28	0.98	UCU(Ser1)	135	39.46	0.43
UUC(Phe)	12	3.51	0.02	UCC(Ser1)	4	1.17	0.01
UUA(Leu1)	99	28.94	0.22	UCA(Ser1)	3	0.88	0.01
UUG(Leu1)	317	92.66	0.69	UCG(Ser1)	9	2.63	0.03
CUU(Leu2)	20	5.85	0.04	CCU(Pro)	55	16.08	0.77
CUC(Leu2)	0	0	0	CCC(Pro)	2	0.58	0.03
CUA(Leu2)	3	0.88	0.01	CCA(Pro)	3	0.88	0.04
CUG(Leu2)	19	5.55	0.04	CCG(Pro)	11	3.22	0.15
AUU(Ile)	141	41.22	0.94	ACU(Thr)	58	16.95	0.89
AUC(Ile)	9	2.63	0.06	ACC(Thr)	1	0.29	0.02
AUA(Met)	37	10.82	0.26	ACA(Thr)	3	0.88	0.05
AUG(Met)	104	30.4	0.74	ACG(Thr)	3	0.88	0.05
GUU(Val)	269	78.63	0.71	GCU(Ala)	55	16.08	0.71
GUC(Val)	9	2.63	0.02	GCC(Ala)	9	2.63	0.12
GUA(Val)	29	8.48	0.08	GCA(Ala)	5	1.46	0.06
GUG(Val)	73	21.34	0.19	GCG(Ala)	9	2.63	0.12
UAU(Tyr)	196	57.29	0.92	UGU(Cys)	117	34.2	0.93
UAC(Tyr)	17	4.97	0.08	UGC(Cys)	9	2.63	0.07
UAA(*)	3	0.88	0.38	UGA(Trp)	23	6.72	0.28
UAG(*)	5	1.46	0.63	UGG(Trp)	58	16.95	0.72
CAU(His)	40	11.69	0.87	CGU(Arg)	47	13.74	0.85
CAC(His)	6	1.75	0.13	CGC(Arg)	1	0.29	0.02
CAA(Gln)	15	4.38	0.33	CGA(Arg)	0	0	0
CAG(Gln)	30	8.77	0.67	CGG(Arg)	7	2.05	0.13
AAU(Asn)	89	26.02	0.98	AGU(Ser2)	97	28.35	0.31
AAC(Asn)	2	0.58	0.02	AGC(Ser2)	8	2.34	0.03
AAA(Lys)	19	5.55	0.27	AGA(Ser2)	17	4.97	0.05
AAG(Lys)	51	14.91	0.73	AGG(Ser2)	40	11.69	0.13
GAU(Asp)	72	21.05	0.9	GGU(Gly)	144	42.09	0.61
GAC(Asp)	8	2.34	0.1	GGC(Gly)	17	4.97	0.07
GAA(Glu)	19	5.55	0.26	GGA(Gly)	15	4.38	0.06
GAG(Glu)	54	15.78	0.74	GGG(Gly)	62	18.12	0.26
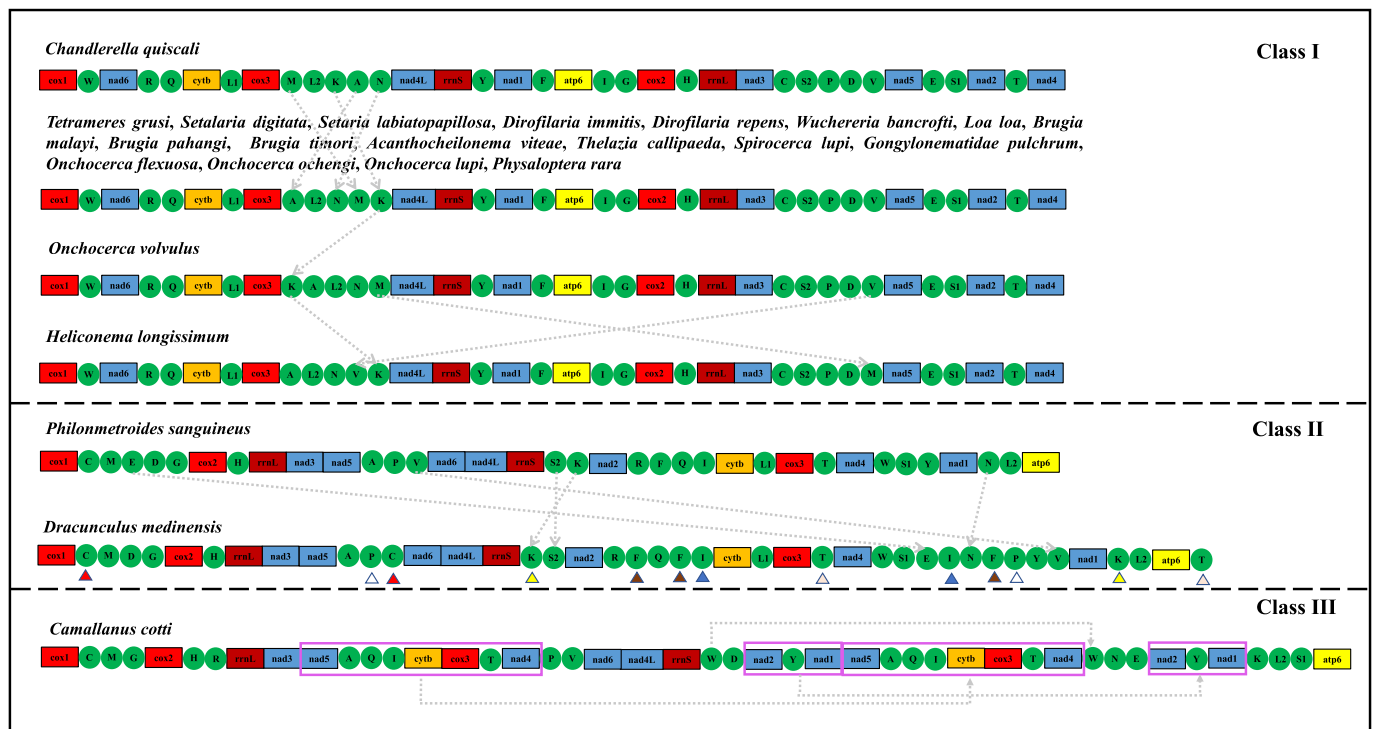
Fig. 2. Mitogenome arrangement in *Tetrameres grusi* compared with those in Spirurina nematodes. The circular mitogenomes were linearized at the 5′ end of *cox*1 gene for illustration purpose. Non-coding regions were not shown. Triangular markers of the same color represent the corresponding duplicated genes. The purple frames represent the duplicated gene fragments.

76.76% (Table 2). *Rrn*L was located between *trn*H and *nad*3, and *rrn*S was located between *nad*4L and *trn*Y. The *rrn*L and *rrn*S genes were 961 bp and 687 bp in *T. grusi*, respectively (Table 1), and they had AT

contents of 76.69% and 75.25%, respectively.

The predicted secondary structures of the 22 tRNAs in *T. grusi* were similar to those of all the Spirurina nematodes examined to date
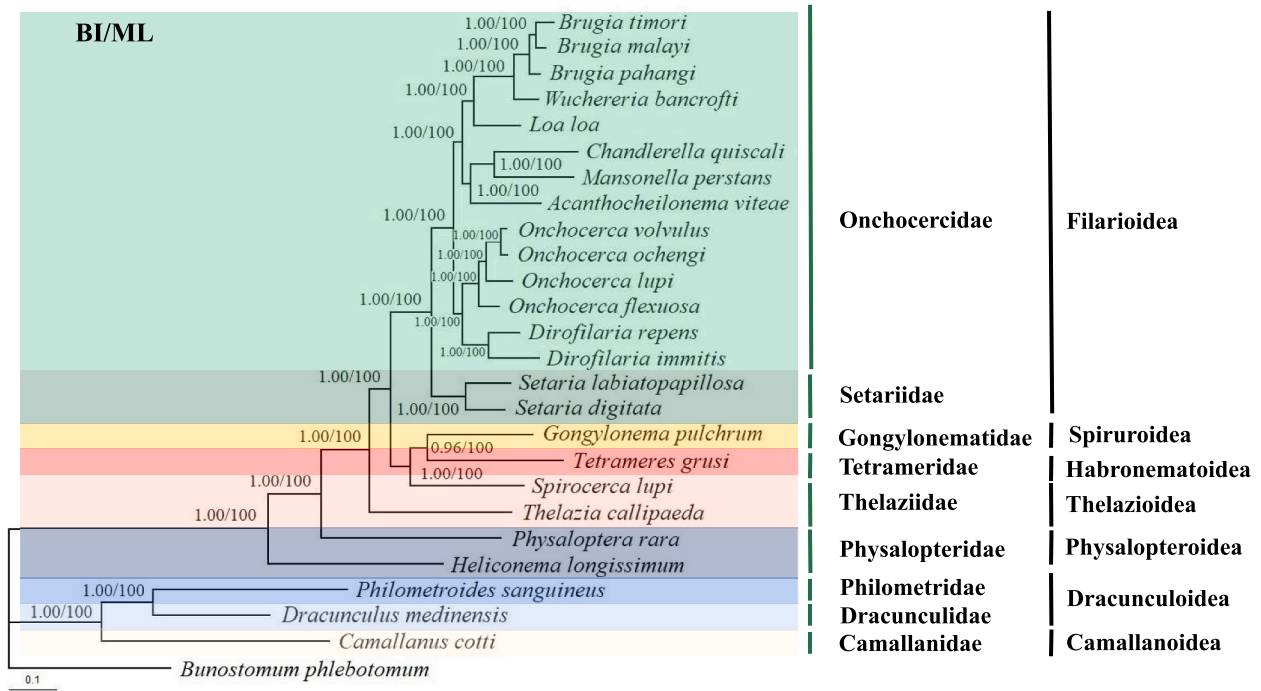
Fig. 3. Phylogenetic relationships of *Tetrameres grusi* with other 24 Spirurina species based on concatenated amino acid sequences of 12 PCGs analyzed by BI and ML using *Bunostomum phlebotomum* as outgroup. Posterior probability values are indicated.

(Fig. S2). The locations of the tRNAs in *T. grusi* were consistent with a majority of Spirurina, except for those of *C. quiscali*, *O. flexuosa*, and *H. longissimum* (Park et al., 2011; McNulty et al., 2012).

The mitogenome of *T. grusi* contains only one NCR, an AT-rich region, having 78.2% AT content (Table 2), which was located between *cox*3 and *trn*A (Fig. 1; Table 1). This result is consistent with some Spirurina, but differs from other nematodes, such as *Ascaris suum* (Liu et al., 2012) and *B. phlebotomum* (Gao et al., 2014), which have two significantly different sized NCRs.

3.4. Gene rearrangements

Gene rearrangements in nematode mitogenomes commonly occur and are used to study phylogenetic relationships. To determine the occurrence of arrangements in *T. grusi*, we compared the gene order of the *T. grusi* mitogenome with those of 24 Spirurina species. The circular mitogenomes were linearized at the 5' end of their *cox*1 genes in the H−strand direction to determine the gene orders of Spirurina species. The sequenced mitogenomes of the 25 Spirurina nematodes showed three classes of gene arrangements based on the 12 PCGs (Fig. 2).

Among the gene arrangements, class I contained 22 Spirurina nematodes that shared an identical arrangement based on 12 PCGs (the order: *cox*1 > *nad*6 > *cyt*b > *cox*3 > *nad*4L > *rrn*S > *nad*1 > *atp*6 > *cox*2 > *rrn*L > *nad*3 > *nad*5 > *nad*2 > *nad*4), but the gene rearrangement events occurred in transposed tRNAs. The gene arrangements in the mitogenomes of nematodes have previously been divided into 26 types (Liu et al., 2013; Deng et al., 2021b). Here, four types of gene arrangements were identified within Spirurina (Fig. 2). In total, 18 out of 24 Spirurina nematodes, *T. grusi*, *S. digitata*, *S. labiatopapillosa*, *D. immitis*, *D. repens*, *W. bancrofti*, *L. loa*, *B. malayi*, *B. pahangi*, *B. timori*, *A. viteae*, *T. callipaeda*, *S. lupi*, *G. pulchrum*, *O. flexuosa*, *O. ochengi*, *O. lupi*, and *P. rara*, had identical gene arrangements, classified as GA9 type. *C. quiscali*, *O. volvulus*, and *H. longissimum* belonged to the GA8, GA10, and GA11 types, respectively. The rearrangement events mainly occurred in two regions of the mitogenome, between *cox*3 and *nad*4L and between *nad*3 and *nad*5. In comparison with the GA9 type, four

tRNAs (*trn*M, *trn*K, *trn*A and *trn*N) were transposed to between *cox*3 and *nad*4L in the GA8 type. In comparison with the GA10 type, *trn*K was transposed to between *cox*3 and *nad*4L in the GA11 type, whereas *trn*M, which is between *cox*3 and *nad*4L in the GA10 type, was transposed to between *nad*3 and *nad*5 in the GA11 type. Additionally, *trn*V, which is between *nad*3 and *nad*5 in the GA10 type, was transposed to between *cox*3 and *nad*4L in the GA11 type.

For the Class II gene arrangement, *P. sanguineus* and *D. medinensis* shared an identical arrangement based on 12 PCGs (the order: *cox*1 > *cox*2 > *rrn*L > *nad*3 > *nad*5 > *nad*6 > *nad*4L > *rrn*S > *nad*2 > *cyt*b > *cox*3 > *nad*4 > *nad*1 > *atp*6). However, four tRNAs (*trn*S2, *trn*K, *trn*E, and *trn*V) existed, and the tRNA transposition phenomenon occurred between *P. sanguineus* and *D. medinensis*, resulting in gene rearrangements. Notably, six tRNAs were duplicated in the *D. medinensis* mitogenome, *trn*F (3), *trn*I (2), *trn*T (2), *trn*P (2), *trn*K (2), and *trn*C (2).

For the Class III gene arrangement, *C. cotti* was the only member (the order: *cox*1 > *cox*2 > *rrn*L > *nad*3 > *nad*5 > *cyt*b > *cox*3 > *nad*4 > *nad*6 > *nad*4L > *nad*2 > *nad*1 > *nad*5 > *cyt*b > *cox*3 > *nad*4 > *nad*2 > *nad*1 > *atp*6). The rearrangement in the *C. cotti* mitogenome contained 46 genes, including six PCGs (*cox*3, *cyt*b, *nad*1, *nad*2, *nad*4, and *nad*5) and six tRNAs (*trn*A, *trn*I, *trn*Q, *trn*T, *trn*W, and *trn*Y) that were duplicated, and these duplicated genes were concentrated in two fragments (*nad*5−*trn*A−*trn*Q−*trn*I−*cyt*b−*cox*3−*trn*T−*nad*4 and *nad*2−*trn*Y−*nad*1), except *trn*W. Additionally, *trn*F, *trn*L1, and *trn*S2 were absent from the *C. cotti* mitogenome.

3.5. Phylogenetic analyses

In the present study, BI and ML approaches were used to estimate the phylogenetic position of *T. grusi* within 24 spirurid nematodes on the basis of the concatenated amino acid sequences of 12 PCGs. Both the methods produced nearly identical tree topologies (Fig. 3).

The topological structures of the phylogenetic trees divided the Spirurina into two clades. Filarioidea, Spiruroidea, Habronematoidea, Thelazioidea, and Physalopteroidea were grouped together form a major clade, whereas Dracunculoidea and Camallanoidea form the other clade.

Our results revealed that Filarioidea, including Onchocercidae and Setariidae, formed a clade with a high nodal support value (ML/BI = 100/1.00). *T. grusi* (Habronematoidea) was sister to *G. pulchrum* (Spiruroidea), and together they formed a clade with *S. lupi* (Thelazioidea). In spite of *S. lupi* and *T. callipaeda* belongs to the superfamily Thelazioidea, bur *T. callipaeda* did not clustered together with *S.lupi* instead of it showed an early diverging position to *S.lupi* in our study. The results were identical to those previously reported using a smaller number of mitogenome and SSU rRNA sequences (Nadler et al., 2007; Liu et al., 2015).

Zou et al. (2017) conducted structural and phylogenomic comparative analyses on Spirurina utilizing complete mitogenome datasets. Their topology of the Spirurina clade indicated that *S. lupi* is closely related to *G. pulchrum* and therefore the authors concluded that it should belong to the family Gongylonematidae (Zou et al., 2017). Interestingly, the controversial taxonomy within Spirurina was also observed in present study, that *G. pulchrum* formed a sister group to *T. grusi*, and together they formed a clade with *S. lupi*. Based on our results, one can either allocate the three species (*G. pulchrum*, *T. grusi*, and *S. lupi*) to the same family, or allocate *G. pulchrum* and *T. grusi* to the same family, sister to *S. lupi*, or allocate each species to its own family.

The phylogenetic relationships of the genus *Tetrameres* (*T. fissipina*) have been previously investigated using nuclear SSU rRNA sequences, showing that *T. fissipina* was closer to the *Onchoceridae sp.*, a kind of free-living filarial worm belong to Filarioidea, than *Thelazia lacrymalis* (Thelazioidea) and *S. lupi* (Thelazioidea) (Nadler et al., 2007). Whereas, the clade formed by *G. pulchrum*, *T. grusi*, and *S. lupi* were more closely related to the Filarioidea family than *T. callipaeda* (Thelazioidea) using mitogenome sequences in present study. Thus, the evolutionary relationship of the genus *Tetrameres* within Spirurina remains unclear absolutely owing to the scarcity of full mitogenome sequences, and more nematode mitogenomes need to be sequenced and then, the evolutionary relationships among these nematodes should be reexamined.

4. Conclusions

In conclusion, we reported the complete mitogenome sequence of *T. grusi* and used the characterization of this mitogenome to reassess the systematic relationships within the suborder Spirurina. Our phylogenetic analyses suggested that *T. grusi* (Habronematoidea) was more closely related to *G. pulchrum* (Spiruroidea) than *S. lupi* (Thelazioidea). It is anticipated that additional taxonomic samplings will provide more reliable information for determining mitogenome evolution and developing better phylogenetic hypotheses for spirurid nematodes evolution.

Declaration of competing interest

The authors report no conflicts of interests.

Appendix A. Supplementary data

Supplementary data to this article can be found online at https://doi.org/10.1016/j.ijppaw.2021.12.001.

References

Agüero, M.L., Gilardoni, C., Cremonte, F., Diaz, J.I., 2016. Stomach nematodes of three sympatric species of anatid birds off the coast of Patagonia. J. Helminthol. 90, 663–667.

Altschul, S.F., Madden, T.L., Schäffer, A.A., Zhang, J., Zhang, Z., Miller, W., Lipman, D.J., 1997. Gapped BLAST and PSI-BLAST: a new generation of protein database search programs. Nucleic. Acids. Res. 25, 3389–3402.

Amundson, C.L., Traub, N.J., Smith-Herron, A.J., Flint, P.L., 2016. Helminth community structure in two species of arctic-breeding waterfowl. Int. J. Parasitol. Parasites. Wildl. 5, 263–272.

Bernt, M., Donath, A., Jühling, F., Externbrink, F., Florentz, C., Fritzsch, G., Pütz, J., Middendorf, M., Stadler, P.F., 2013. MITOS: improved de novo metazoan mitochondrial genome annotation. Mol. Phylogenet. Evol. 69, 313–319.

Darriba, D., Taboada, G.L., Doallo, R., Posada, D., 2012. jModelTest 2: more models, new heuristics and high-performance computing. Nat. Methods. 9, 772.

de Ley, P., Blaxter, M.L., 2004. A new system for nematoda: combining morphological characters with molecular trees, and translating clades into ranks and taxa. Proc. Fourth. Int. Congr. Nematol. 2, 633–653.

de Lima, P.H.C., Barcelos, R.M., Klein, R.C., Vidigal, P.M.P., Montandon, C.E., Fabres-Klein, M.H., Dergam, J.A., Mafra, C., 2017. Sequencing and comparative analysis of the *Amblyomma sculptum* mitogenome. Vet. Parasitol. 247, 121–128.

Deng, Y.P., Zhang, X.L., Li, L.Y., Yang, T., Liu, G.H., Fu, Y.T., 2021a. Characterization of the complete mitochondrial genome of the swine kidney worm *Stephanurus dentatus* (Nematoda: Syngamidae) and phylogenetic implications. Vet. Parasitol. 295, 109475.

Deng, Y.P., Suleman, Zhang, Y., Nie, Y., Fu, Y.T., Liu, G.H., 2021b. The complete mitochondrial genome of *capillariid nematodes* (Eucoleus annulatus): a novel gene arrangement and phylogenetic implications. Vet. Parasitol. 296, 109476.

Diaz, J.I., Fusaro, B., Longarzo, L., Coria, N.R., Vidal, V., Jerez, S., Ortiz, J., Barbosa, A., 2013. Gastrointestinal helminths of Gentoo penguins (Pygoscelis papua) from stranger point, 25 de Mayo/King George Island, Antarctica. Parasitol Res 112, 1877–1881.

Dierckxsens, N., Mardulyn, P., Smits, G., 2017. NOVOPlasty: de novo assembly of organelle genomes from whole genome data. Nucleic. Acids. Res. 45, e18.

Edgar, R.C., 2004. MUSCLE: multiple sequence alignment with high accuracy and high throughput. Nucleic. Acids. Res. 32, 1792–1797.

Fink, M., Permin, A., Magwisha, H.B., Jensen, K.M., 2004. *Tetrameres americana* Cram (1927) populations in chickens infected with different dose levels. Vet. Parasitol. 124, 239–247.

Gao, J.F., Zhao, Q., Liu, G.H., Zhang, Y., Zhang, Y., Wang, W.T., Chang, Q.C., Wang, C.R., Zhu, X.Q., 2014. Comparative analyses of the complete mitochondrial genomes of the two ruminant hookworms *Bunostomum trigonocephalum* and *Bunostomum phlebotomum*. Gene 541, 92–100.

Gao, J.F., Zhang, X.X., Wang, X.X., Li, Q., Li, Y., Xu, W.W., Gao, Y., Wang, C.R., 2019. According to mitochondrial DNA evidence, Parascaris equorum and Parascaris univalens may represent the same species. J. Helminthol. 93, 383–388.

Gao, Y., Wang, X.X., Ma, X.X., Zhang, Z.H., Lan, Z., Qiu, Y.Y., Wang, S., Song, M.X., Wang, C.R., 2021. Characterization of the complete mitochondrial genomes of *Coronocyclus labiatus* and *Cylicodontophorus bicoronatus*: comparison with Strongylidae species and phylogenetic implication. Vet. Parasitol. 290, 109359.

González-Acuña, D., Veloso-Frías, J., Missene, C., Oyarzún-Ruiz, P., Fuentes-Castillo, D., Kinsella, J.M., Mironov, S., Barrientos, C., Cicchino, A., Moreno, L., 2020. External and gastrointestinal parasites of the Franklin's Gull, *Leucophaeus pipixcan* (Charadriiformes: Laridae), in Talcahuano, central Chile. Rev. Bras. Parasitol. Vet. 29, e016420.

Hodda, M., 2011. Phylum nematoda Cobb 1932. Zootaxa 3148, 63–95.

Honisch, M., Krone, O., 2008. Phylogenetic relationships of Spiruromorpha from birds of prey based on 18S rDNA. J. Helminthol. 82, 129–133.

Hu, M., Gasser, R.B., Abs El-Osta, Y.G., Chilton, N.B., 2003. Structure and organization of the mitochondrial genome of the canine heartworm, *Dirofilaria immitis*. Parasitology 127, 37–51.

Hu, L., Zhang, M., Sun, Y., Bu, Y., 2020. Characterization and phylogenetic analysis of the first complete mitochondrial genome of *Cylicocyclus radiatus*. Vet. Parasitol. 281, 109097.

Huelsenbeck, J.P., Ronquist, F., 2001. MRBAYES: Bayesian inference of phylogenetic trees. Bioinformatics 17, 754–755.

Królaczyk, K., Kavetska, K.M., Dzierzba, E., Stapf-Skiba, A., 2018. *Tetrameres globosa* (Linstow, 1879) (Nematoda, Tetrameridae) – a nematode of the Eurasian coot Fulica atra (Linnaeus, 1758) recorded for the first time in Poland. Ann. Parasitol 64, 137–141.

Liu, G.H., Wu, C.Y., Song, H.Q., Wei, S.J., Xu, M.J., Lin, R.Q., Zhao, G.H., Huang, S.Y., Zhu, X.Q., 2012. Comparative analyses of the complete mitochondrial genomes of *Ascaris lumbricoides* and *Ascaris suum* from humans and pigs. Gene 492, 110–116.

Liu, G.H., Wang, Y., Song, H.Q., Li, M.W., Ai, L., Yu, X.L., Zhu, X.Q., 2013. Characterization of the complete mitochondrial genome of *Spirocerca lupi*: sequence, gene organization and phylogenetic implications. Parasit. Vectors 6, 45.

Liu, G.H., Jia, Y.Q., Wang, Y.N., Zhao, G.H., Zhu, X.Q., 2015. The complete mitochondrial genome of the gullet worm Gongylonema pulchrum: gene content, arrangement, composition and phylogenetic implications. Parasit. Vectors 8, 100.

Lohse, M., Drechsel, O., Kahlau, S., Bock, R., 2013. OrganellarGenomeDRAW—a suite of tools for generating physical maps of plastid and mitochondrial genomes and visualizing expression data set. Nucleic. Acids. Res. 41, W575–W581.

McNulty, S.N., Mullin, A.S., Vaughan, J.A., Tkach, V.V., Weil, G.J., Fischer, P.U., 2012. Comparing the mitochondrial genomes of Wolbachia-dependent and independent filarial nematode species. BMC Genomics 113, 145.

Mowlavi, G.R., Massoud, J., Mobedi, I., Gharagozlou, M.J., Rezaian, M., Solaymani-Mohammadi, S., 2006. *Tetrameres* (Tetrameres) *grusi* (Shumakovich, 1946) (nematoda: Tetrameridae) in Eurasian cranes (Grus grus) in central Iran. J. Wildl. Dis. 42, 397–401.

Mukaratirwa, S., Khumalo, M.P., 2010. Prevalence of helminth parasites in free-range chickens from selected rural communities in KwaZulu-Natal province of South Africa. J. S. Afr. Vet. Assoc. 81, 97–101.

Nadler, S.A., Carreno, R.A., Mejía-Madrid, H., Ullberg, J., Pagan, C., Houston, R., Hugot, J.P., 2007. Molecular phylogeny of clade III nematodes reveals multiple origins of tissue parasitism. Parasitology 134, 1421–1442.

Olsen, A.C., Fedynich, A.M., 2016. Helminth infections in northern bobwhites (colinus virginianus) from a legacy landscape in Texas, USA. J. Wildl. Dis. 52, 576–581.

Padilla-Aguilar, P., Romero-Callejas, E., Ramírez-Lezama, J., Osorio-Sarabia, D., García-Prieto, L., Manterola, C., García-Márquez, L.J., Zarza, H., 2020. Gastrointestinal helminths of waterfowl (Anatidae: Anatinae) in the Lerma marshes of central Mexico: some pathological aspects. Int. J. Parasitol. Parasites. Wildl. 13, 72–79.

Park, J.K., Sultana, T., Lee, S.H., Kang, S., Kim, H.K., Min, G.S., Eom, K.S., Nadler, S.A., 2011. Monophyly of clade III nematodes is not supported by phylogenetic analysis of complete mitochondrial genome sequences. BMC Genomics 12, 392.

Perna, N.T., Kocher, T.D., 1995. Patterns of nucleotide composition at fourfold degenerate sites of animal mitochondrial genomes. J. Mol. Evol. 41, 353–358.

Pyziel, A.M., Laskowski, Z., Dolka, I., Kołodziej-Sobocińska, M., Nowakowska, J., Klich, D., Bielecki, W., Żygowska, M., Moazzami, M., Anusz, K., Höglund, J., 2020. Large lungworms (Nematoda: Dictyocaulidae) recovered from the European bison may represent a new nematode subspecies. Int. J. Parasitol. Parasites Wildl. 13, 213–220.

Rombel, I.T., Sykes, K.F., Rayner, S., Johnston, S.A., 2002. ORF-FINDER: a vector for high throughput gene identification. Gene 282, 33–41.

Schou, T.W., Permin, A., Juul-Madsen, H.R., Sørensen, P., Labouriau, R., Nguyên, T.L., Fink, M., Pham, S.L., 2007. Gastrointestinal helminths in indigenous and exotic chickens in Vietnam: association of the intensity of infection with the Major Histocompatibility Complex. Parasitology 134, 561–573.

Soulsby, E.J.L., 1982. In: Helminths, Arthropods, and Protozoa of Domesticated Animals, seventh ed. Bailiere Tindall, London, UK, p. P809.

Stamatakis, A., 2014. RAxML version 8: a tool for phylogenetic analysis and post-analysis of large phylogenies. Bioinformatics 30, 1312–1313.

Tamura, K., Stecher, G., Kumar, S., 2021. MEGA11: molecular evolutionary genetics analysis version 11. Mol. Biol. Evol. 38, 3022–3027.

Werneck, M.R., Jerdy, H., Ribeiro, R.B., Bianchi, M., Maciel, L.L.F., de Aquino Almeida, J.C., Baldassin, P., Gallo, H., Carvalho, E.C.Q., 2020. Atrophic proventriculitis associated with Gravid females of *Tetrameres* sp. (nematoda: Tetrameridae) in the Magellanic penguin (*Spheniscus magellanicus*) on the coast of Brazil. J. Parasitol. 106, 180–183.

Yatawara, L., Wickramasinghe, S., Rajapakse, R.P., Agatsuma, T., 2010. The complete mitochondrial genome of *Setaria digitata* (Nematoda: Filarioidea): mitochondrial gene content, arrangement and composition compared with other nematodes. Mol. Biochem. Parasitol. 173, 32–38.

Zou, H., Jakovlić, I., Chen, R., Zhang, D., Zhang, J., Li, W.X., Wang, G.T., 2017. The complete mitochondrial genome of parasitic nematode *Camallanus cotti*: extreme discontinuity in the rate of mitogenomic architecture evolution within the Chromadorea class. BMC Genomics 18, 840.